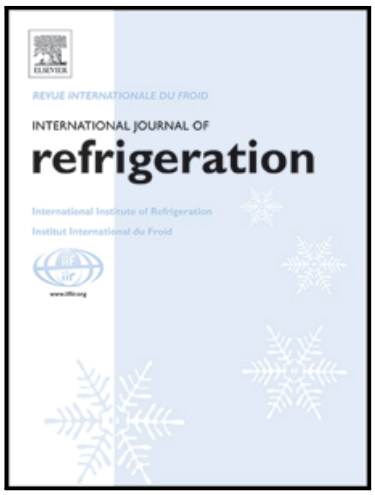

Cooling by sweeping: a new operation method to achieve ferroic refrigeration without fluids or thermally switchable components

D.J. Silva, J.S. Amaral, V.S. Amaral

PII: S0140-7007(19)30079-9
DOI: https://doi.org/10.1016/j.ijrefrig.2019.02.029
Reference: JIJR 4299

To appear in: *International Journal of Refrigeration*

Received date: 3 October 2018
Revised date: 31 January 2019
Accepted date: 22 February 2019

Please cite this article as: D.J. Silva, J.S. Amaral, V.S. Amaral, Cooling by sweeping: a new operation method to achieve ferroic refrigeration without fluids or thermally switchable components, *International Journal of Refrigeration* (2019), doi: https://doi.org/10.1016/j.ijrefrig.2019.02.029

Highlights

- An operation mode for caloric refrigeration, "cooling by sweeping", is presented
- Device heat flow is established by exploiting applied field dynamics
- A simple magnetic refrigerator geometry is considered for validation
- Using this method, no fluids or thermally switchable components are required

Cooling by sweeping: a new operation method to achieve ferroic refrigeration without fluids or thermally switchable components

D. J. Silva[a,1], J. S. Amaral[a], V. S. Amaral[a]

[a] *Department of Physics and CICECO - Aveiro Institute of Materials, University of Aveiro, 3810-193 Aveiro, Portugal*

Abstract

So far, all ferroic-based refrigerator prototypes have relied either in fluids or thermally switchable components as main heat exchangers, which brings some issues in terms of their applicability, such as the use of pumps for moving the fluid and the availability of thermally switchable components. We show that such heat exchangers are not necessary if field dynamics are explored. By using the example of magnetocaloric refrigeration, we show numerically that the operation of a simple apparatus constituted only by a magnetocaloric material and a magnet sweeping at a given frequency results in refrigeration. With the optimization of the type of motion, resting times after the complete application and removal of the magnetic field and frequency, a temperature span of 0.87 K is reached, which represents $\sim 20\%$ of the maximum adiabatic temperature span of the material used in modeling, gadolinium.

Keywords: Solid state refrigeration, Ferroic refrigeration, Magnetocaloric effect, Magnetic field

Email address: djsilva@ua.pt, Phone: +351 234 370 356, Fax: +351 234 378 197 (D. J. Silva)

Nomenclature

Roman

C	specific heat ($Jkg^{-1}K^{-1}$)
COP	coeficient of performance
H	magnetic field (Am^{-1})
k	thermal conductivity ($Wm^{-1}K^{-1}$)
L	system length (m)
MCM	Magnetocaloric material
N	number of sections
RT	resting time ratio
T	temperature (K)
t	time (s)
x	space (m)

Greek

Δ	difference
ν	frequency (Hz)
ρ	density (kgm^{-3})
τ	sweeping time interval (s)

Subscript

ad	adiabatic
$cold$	after the complete removal of H
H	at constant magnetic field
hot	after the complete application of H
i	space index
max	maximum

Superscript

n	time index

1. Introduction

Refrigeration accounts for a significant share of the world's energy consumption [1]. In this context, the effort on improving the efficiency of the respective systems has been growing significantly. While the vapor-compression technology is still the most used refrigeration technology, the interest for ferroic-based refrigeration has been increasing for the past decades [2, 3], mainly due to the large efficiency when compared to conventional vapor-compression devices since coefficient of performance (COP) values can reach 30%–60% of the Carnot efficiency [1, 4], and due to the absence of nocive gases since the refrigerant can be completely solid.

Among all ferroic-based thermotechnologies, magnetocaloric refrigeration has become one of the most reported alternatives to vapor-compression systems [5–7]. Indeed, magnetocaloric refrigeration has the potential to reduce the energy consumption by more than 20% over vapor-compression systems [1]. The principle of operation relies on the adiabatic magnetization (or demagnetization) of the so called magnetocaloric materials that results in their temperature increase (or reduction) [8, 9]. The recent intensive research on the preparation and characterization of magnetocaloric materials resulted in significant improvements in the performance of prototypes. However, magnetocaloric refrigerators have been limited to a few number of designs and operation modes [10–17]. Most of the designs include fluids behaving as main heat exchangers and use the magnetocaloric material itself as active regenerator, in some cases using the effect of tapering, so that the temperature span is not limited to the maximum adiabatic temperature variation upon the application or removal of magnetic fields. Heat is thus flown through the

magnetocaloric material (by conduction) and through the fluid (by conduction and convection). Other systems have been proposed to operate with thermally switchable components as main heat exchangers, such as thermal diodes, thermal regulators or thermal switches, still with a fluid as important ingredient [18–20]. Only a few number of geometries have allowed the complete removal of fluids [21–24]. In these systems, heat flows entirely within the magnetocaloric material by heat conduction. The active magnetic regeneration in such fully solid state magnetic systems can be performed with the use of a gradual demagnetization from the hot end to the cold end [22].

Overall, room temperature ferroic-based refrigeration has been achieved by using fluids or thermally switchable components as main heat exchangers [7, 18, 21, 25–28], which brings some issues in terms of their applicability, such as the use of pumps for moving the fluid [29], which reduces significantly the total efficiency of the system, and the availability of thermally switchable components [23, 24]. Finding suitable macroscopic thermally switchable component, such as thermal diodes, thermal regulators or thermal switches, with a considerable durability has been a huge challenge [30, 31]. While some nanostructured devices already have thermal switchable properties when activating with external fields, e.g. Co/Cu multilayers when the external field is the magnetic field [32], they are not appropriate for macroscopic setups due to the very small thermal axial time response. Peltier devices can be used to mimic thermal switchable behaviors [18, 33, 34], however their functioning need an additional and significant power source which degrades the final efficiency. Thermal diodes, such as PNIPAM/PDMS [35], are another possibility but the respective thermal rectification is too small when compared with

the relative change of the effective thermal conductivity of thermal switches. More complex systems exist such as devices constituted by nanofluids [36] or mechanically activated devices [37], however independent field systems need to be included due to the cyclical operation of the system. In summary, thermally switchable components can be considered as a solution but there are still a quite long journey ahead.

In this work we propose a new design that excludes the use of fluids or thermally switchable components as main heat exchangers, and we test the operation by using the example of magnetocaloric refrigeration. In the proposed system the heat flows only through the magnetocaloric material, in a direction that is dictated by the motion of the magnet, i.e. by the heterogeneous variation of the magnetic field. We demonstrate the possibility to achieve magnetocaloric refrigeration by using 49 operation modes that combine several types of accelerated motions, and different resting times after fully applying and removing the magnetic field. The general concept of cooling by sweeping for other caloric effects is described.

2. Concept

The fully solid state magnetocaloric refrigerator that is considered in the following is represented in Fig. 1 (a). The system consists of a magnetocaloric material (MCM) in permanent contact with a cold reservoir. The operation of the system relies on the linear motion of the magnets, represented in black. The magnets can move from left to right and from right to left. Moreover, they can move with constant speed, with accelerated motion or decelerated motion. An ideal case can occur when the magnetic field

(H) is applied instantaneously (abrupt motion of the magnets). The system operates at a fixed frequency ν. Each operation cycle occurs when the whole system reaches a state where H is 0 and another one where H is H_{max}. Figure 1 (b) shows the thermodynamic cycle of the closest sections to the hot and cold reservoirs. Both cycles are not equal, so that a temperature span can arise. However, unlike the well known active magnetic regenerative thermodynamic cycle, the two cycles overlap, which can result in a temperature span below the maximum adiabatic temperature variation upon the application or removal of H. Additional variables that play important roles on the performance of magnetocaloric refrigeration are resting times, that accounts the time spent before the application and removal of H. The following subsections describe the mechanics of the application and removal of H (for constant speed, accelerated motion, and decelerated motion), and resting times.

2.1. Sweeping: $H(x,t)$

The motion of the magnetic field is defined by the sweeping function $H(x,t)$. For simplicity the system is considered to be 1 dimensional, divided by N elements with identical length L/N. It is also assumed that H can only be 0 (removed) or H_{max} (applied) in each element, i.e. the motion is a result of switching the magnetic field from 0 to H_{max} or from H_{max} to 0 in each element, at different times. Hence, in this context the sweeping function $H(x,t)$ is completely discretized:

$$x_i, t_n \rightarrow \{0, H_{max}\}. \tag{1}$$

Considering that we want to apply (or remove) H from the whole length L in a time interval τ at constant speed, the time instant when the application (or removal) of H occurs is

$$t_i = \frac{\tau}{N} + t_{i\mp 1}, \tag{2}$$

where i accounts for each element as shown in Fig. 1 **(a)** and takes the values $i = 0, 1, 2, ..., N$ if the motion takes place from left to right, and $i = N, N-1, N-2, ..., 1$ if the motion occurs from right to left. The sign $\mp$ becomes $-$ for the motion from left to right and $+$ for the motion from right to left. If the motion is performed in an accelerated manner the time instant when the application (or removal) of H occurs is

$$t_i = \frac{\tau}{\sqrt{N}}(\sqrt{j} - \sqrt{j-1}) + t_{i\mp 1}, \tag{3}$$

where $j = i$ if the motion occurs from left to right, and $j = N - i$ if the motion occurs from right to left. In the same manner, if we are using a decelerated motion, the time instant when the application (or removal) of H occurs is:

$$t_i = \frac{\tau}{\sqrt{N}}(\sqrt{N-j+1} - \sqrt{N-j}) + t_{i\mp 1}. \tag{4}$$

The equivalent motion of the magnets can be visualized in Fig. 1 **(b)** for the application of H and in Fig. 1 **(c)** for the removal of H. Equations 3 and 4 were obtained with simple classical mechanics by applying the equations of motion to the magnetic field H.

2.2. Resting times

The magnets perform two forms of motion: application of H and removal of H. Between these movements, H stays static over a period of time,

hereafter referenced to as resting time. There are two time intervals that corresponds to resting times: when the whole system is under the magnetic field H_{max}, and when the whole system is under a 0 magnetic field. These two resting times occur before the removal of H (hot resting time ratio, RT_{hot}) and before the application of H (cold resting time ratio, RT_{cold}). These ratios are relative to the cycle period. For a fixed frequency ν, these resting times will influence the time interval τ used when sweeping the magnetic field within a cycle:

$$\tau = \frac{1}{2\nu}(1 - RT_{cold} - RT_{hot}). \tag{5}$$

Note that these resting times dictate the time the cold reservoir is in contact to the MCM at a low or high temperature.

3. Model

The used model for each cycle is divided in several procedures shown in Fig. 2. First several inputs are given, which includes the materials properties and the discretization of all the state variable and materials properties by fixing the space and time steps Δx and Δt. The operation starts with the demagnetization of the system at a specific mode Y, that will be described in subsection 3.2. Once the magnetic field is 0 in the whole system, it evolves during a time interval (cold resting time). Afterwards, the magnetization occurs in the mode X, that will be described in subsection 3.2 as well. Once the magnetic field is H_{max} in the whole system, thermal processes occur during a time interval (hot resting time). Finally, a comparison of the temperature of the middle of the cold reservoir is done and if the difference is below a

given value the simulation stops and an output, that includes the space and time evolution of temperature, is given, otherwise the simulation continues with a new cycle. In this section the mathematical model of the used solver is described, as well as the operation of the simulated system.

3.1. heat conduction and magnetocaloric effect

Since the system does not include fluids, and neglects thermal processes by radiation, only heat conduction is considered. Moreover, the system under study is a simple solid bar made of magnetocaloric material, so that the heat conduction equation can be simplified to the equivalent 1 dimensional equation [38–40]:

$$C\frac{\partial T}{\partial t} - \frac{\partial}{\partial x}\left(k\frac{\partial T}{\partial x}\right) = 0, \tag{6}$$

where $C = \rho C_H$, ρ is the density, C_H the specific heat at constant H, k the heat conduction, t the time, x the position, and T the temperature. Note that since we are using different materials for the reservoir and MCM one cannot take the thermal conductivity k out of the space derivative, as is done recurrently in similar problems.

The numerical simulation of this equation was performed with the finite difference method with the so called implicit Crank-Nicholson method. The discretization was performed by dividing the time and space in equal pieces. In this context, the indexes i and n correspond to space and time respectively. Hence, T_i^n corresponds to the temperature for time n and space i. Two consecutive points are thus separated by Δx, for space, and Δt, for time. The calculation of the temperature in all elements in each discrete time is

done by solving the matrix described by

$$\begin{aligned} &-(k_{i-1}^{n+1}+k_i^{n+1})T_{i-1}^{n+1}+\\ &(\gamma_i+k_{i+1}^{n+1}+2k_{i-1}^{n+1})T_i^{n+1}-\\ &(k_{i+1}^{n+1}+k_i^{n+1})T_{i+1}^{n+1}=\\ &=(k_{i-1}^{n+1}+k_i^{n+1})T_{i-1}^{n}+\\ &(\gamma_i-k_{i+1}^{n+1}-2k_i^{n+1}-k_{i-1}^{n+1})T_i^{n}+\\ &(k_{i+1}^{n+1}+k_i^{n+1})T_{i+1}^{n}, \end{aligned} \tag{7}$$

where $\gamma=\frac{4\rho_i^{n+1}C_{p_i}^{n+1}\Delta x^2}{\Delta t}$.

The magnetocaloric effect is guaranteed by changing the temperature at the instant in question according to the adiabatic change of temperature of the material:

$$T_i^{n+1}=T_i^n\pm\Delta T_{ad}^{\pm}(T_i^n), \tag{8}$$

where the + and - signs accounts for the application and removal of H, respectively, so that ΔT_{ad}^{+} and ΔT_{ad}^{-} correspond to the adiabatic temperature change when applying and removing the H, respectively.

In this work, the performance of the refrigerator will be based on the temperature span defined by

$$\Delta T=T_{amb}-T_{cold}, \tag{9}$$

where T_{amb} is the room temperature and T_{cold} is the temperature at the cold reservoir.

3.2. boundary conditions and operation mode

In order to obtain a realistic approach, the simulated system evolves with the hot end in thermal contact with the ambient that is at 293 K ($T(x=$

$0, t) = 293K$). The cold reservoir is considered to be in thermal contact with the magnetocaloric material in one of the two borders and is insulated at the other border (at $x = x_{max}$). The thermal insulation at the cold reservoir is computed by taking the first derivative to be equal to zero:

$$\left(\frac{\partial T}{\partial x}(x,t)\right)_{x_{max}} = 0. \tag{10}$$

The whole system is at the ambient temperature of 293 K at $t = 0$ s.

As described in section 2, the movement of the magnetic field can follow several approaches. To simplify, we picked 3 types of motion: constant velocity, accelerated motion and decelerated motion. For each type the magnets can move from left to right and from right to left. Additionally, the application or removal of H can be instantaneous. Overall, 7 operation modes are considered as shown in Tab. 1. Figure 3 illustrates how the application of H occurs for mode 2. The motion of the magnets is described in more detail in Fig. 1 **(b)** and **(c)**. For the simplicity of the description we say that the system operates in mode XY when the H-application is done in mode X and the H-removal is done in mode Y. Note that there are a total of 49 combinations of operating modes. The described model was implemented in an optimized python2.7 package named *heatrapy* (heat transfer python package, version v0.1.4) [41, 42]. The *heatrapy* package has been validated by comparing solid state heat transfer processes with the COMSOL multiphysics software [42].

For all performed simulation, pure gadolinium (Gd) was considered as the MCM. The temperature dependence of the adiabatic change of temperature upon the removal and application of a magnetic field of 1 T, and the specific heat at 0 and 1 T were calculated using: the Weiss mean field model for

Table 1: Modes for the application and removal of H.

Mode	Process of applying and removing H
0	instantaneous
1	constant velocity from left to right
2	constant acceleration from left to right
3	constant deceleration from left to right
4	constant velocity from right to left
5	constant acceleration from right to left
6	constant deceleration from right to left

the heat capacity and magnetism, Debye model for the lattice heat capacity, and Sommerfeld model for the electronic heat capacity [43]. The Curie temperature is 294 K. The used thermal conductivity and density for Gd was 10.5 W/(m K) and 7900 Kgm^{-3}. Finally, the cold reservoir is made of copper (Cu), so that the adiabatic temperature change upon the removal and application of a magnetic field of 1 T was considered to be 0. The used thermal conductivity, specific heat and density were 401 W/(m K), 385 J/(Kg K) and 8933 Kgm^{-3}. The whole system has a length of 6.5 cm: 5 cm of magnetocaloric material and 1.5 cm of cold reservoir.

By using Δt=0.01s and Δx=0.001m, each performed simulation lasted approximately 10 minutes, which resulted from a steady state condition in which the relative change of the average temperature of the cold reservoir is below 1x10^{-8}. We note that such Δt and Δx values were used following

a previous study on the more adequate value that result on convergence. As mentioned above, 49 mode combinations were considered for the operating frequency of 0.1 Hz, which was chosen after a first assessment on the frequency that resulted in the largest temperature span. Adding the used different resting time ratios (55) one arrives at a number of 2695 simulations. Summing the validation simulations described below we end up with 5418 simulations. Since each performed simulation lasted approximately 10 min in a single core from the used processor Intel(R) Core(TM) i7-3770K CPU @ 3.50GHz, the computation time required to complete all simulations was 38 days.

4. Results

The largest temperature span was achieved for the operating mode 56, cold resting time ratio of 0.5 and hot resting time ration of 0.0. The time evolution of the middle of the cold reservoir is shown in Fig. 4. One can observe that the temperature of the cold reservoir reduces until reaching a stationary state where the temperature bounces between 291.97 K and 292.47 K. However, the average temperature is 292.13 K, which corresponds to a temperature span of 0.87 K. This value is $\sim$ 20% the maximum adiabatic temperature variation of gadolinium under 1 T of applied magnetic field and temperature of 294 K (Curie temperature).

The fact that a temperature span is obtained might not mean that we are in the presence of refrigeration. For instance, the temperature span can come from the fact that the system starts with a demagnetization, which reduces the temperature of the cold reservoir at once and stays there without

transferring heat from the cold reservoir to the magnetocaloric material. To validate the performed simulations, 3 procedures were taken into account, which are described below.

1. The cooling power must tend to zero when approaching to the stationary state, since the CR is ideally insulated from the outside. Notice that no loss is incorporated in the model, so that if the temperature of the cold reservoir reaches a fixed temperature over time, no heat exchanges during a cycle can be observed. This behavior was validated for all the simulations.
2. The final solution cannot depend on the initial temperature of the system, since the hot end is at a fixed temperature. In these conditions, the system may require more, or less, time to reach the stationary state, but the final temperature span has to be the same. Several initial temperatures (289, 291, 293, 295, 297 K) for modes 00, 11, 22, 33, 44, 55, 66 (resting time ratios of 0.0) were tested, and validated.
3. To assure that the temperature span comes from refrigeration and not from the first demagnetization of the operation, all simulations were repeated considering a magnetization process as first step. For the cases where a temperature span was obtained, both demagnetization and magnetization as first steps gave identical solutions. In particular, for the same simulation of Fig. 4 but using magnetization as first step, one can see that the system tends to the same temperature, showing that the system is actually a refrigerator.

Some of the combinations of operating mode and resting time ratios resulted on refrigeration. However, all the operating modes showed several

possible combinations. To summarize the best performance of each operating mode, Fig. 5 shows the largest temperature span of each of the 49 modes, and the corresponding resting time ratios. The temperature spans when using magnetization as first step are identical to the values when using demagnetization, showing that for all these operation parameters, the temperature span is not affected by the fist magnetocaloric effect step, so that all the data shown in Fig. 5 corresponds to refrigerators. The particular case of mode 00, RT_{cold}=0.0 and RT_{hot}=0.0 must result on a zero temperature span, due to the absence of any symmetry. However, a small deviation is found (0.24 K). This value is plotted in Fig. 5 **(a)** and can be considered as a reference for the zero temperature span.

5. Discussion

From Fig. 5 one can easily note that the optimum RT_{cold} tends to be large. The more the system spends its time at a low temperature the more the temperature of the cold reservoir reduces its temperature. However, for most of the modes X0, i.e. those where H is removed instantaneously, a large cold resting time is not required. In fact, the optimum cold resting time ratio is quite low (near 0), which might be due to the absence of the effect of sweeping the magnetic field during the removal of H and thus a longer cold resting time ratio is not needed to optimize the performance. In contrast, the optimized hot resting time ratio follows the same small values for all the shown simulations from Fig. 5, around zero.

The operating modes with the worse temperature span correspond to 0Y, i.e. those where the magnetic field is applied instantaneously. The heat flow

from the magnetocaloric material to the hot reservoir is thus more efficient if using the sweeping of the applied magnetic field. Although the other modes show some differences between them it is clear that the huge step on the temperature span occurs from modes with instantaneous application of H to modes with H sweeping.

The direction of the demagnetization may play a role when applying H from the cold to the hot reservoirs, i.e. for modes 4Y, 5Y and 6Y. As shown in Fig. 5, in these cases the temperature span of the modes X4, X5, and X6 is, in general, larger than the remaining modes. The best performance occurs when the demagnetization takes place from right to left, so that the rightmost element of the magnetocaloric element is mostly at low temperature in one cycle. This operation contrasts with the system of Ref. [22], where the demagnetization occurs from the hot to the cold reservoir. However, in that system, two thermal switches were directing the heat, while the sweeping of the magnetic field was switching on the magnetocaloric material as active magnetic regenerator. In the present case, the sweeping of the magnetic field is directing the heat flow.

Accelerating the sweeping of the demagnetization (modes X2 and X5) shows the worse performance of the refrigerator, however by a small amount compared to the constant velocity and decelerated motion. On the other hand decelerating the sweeping of the magnetization (modes 3Y and 6Y) results on the worse performance, again by a small amount compared to the constant velocity and accelerated motion. The type of motion is thus not the most important parameter to achieve a large temperature span.

These simulations show clearly that refrigeration can be reached without

adding any fluid or thermally switchable component. However, one should mention that losses were excluded from this work, which might be an issue since the frequency is very low so that thermal losses can contribute to reduce significantly the final temperature span. Nevertheless, one might note that the material considered here was not optimized, and neither the dimensions. Using different magnetocaloric materials could have implications on the frequency and thus could reduce the influence of thermal losses on the performance of the refrigerator [8]. Moreover, using a cascade of magnetocaloric materials can increase the temperature span by a considerable amount. Note that the maximum adiabatic temperature change upon the application of H of 1 T of Gd is $\sim$ 4 K and the Curie temperature is $\sim$ 294 K. Using different materials (or compositions) along the magnetocaloric bar, one could improve the efficiency of heat exchanges and, thus, improve the temperature spans [44]. Examples of Curie temperature tunable materials include the magnetocaloric material families $La(Fe, Si)_{13}$ [45, 46], and Fe_2P type [47–49].

Finally, one must note that cooling by sweeping is not confined only to systems based on the magnetocaloric effect, but can be extended to systems with caloric effects in general [2, 3, 50–53]. The motion of the magnetic field can be easily substituted with the motion of the electric field if using the electrocaloric effect [54–56], motion of the stress if using the elastocaloric effect [28, 57–59], or motion of the pressure if using the barocaloric effect [60–63]. Therefore, the general concept of cooling by sweeping can be introduced as a new operation method to achieve fully solid state refrigeration when handling with ferroic materials.

6. Conclusion

In conclusion, we have demonstrated that the use of fluids or thermally switchable components in magnetocaloric refrigerators can be substituted by optimizing magnetic field sweeping to direct the heat flow. The best performance occurs when using large cold resting times, applying the magnetic field from the cold to the hot reservoirs in an accelerated motion, and removing the magnetic field from the colt to the hot reservoirs in a decelerated motion. The most critical parameter to reach refrigeration is the large cold resting time ratio and the sweeping of the applied magnetic field. The maximum temperature span achieved was 0.87 K ($\sim$ 20% of the adiabatic temperature change upon the application of a magnetic field of 1 T of Gd) for the operating mode 56, frequency of 0.1 Hz, cold resting time ratio of 0.5 and hot resting time ratio of 0.0. These values can be easily improved by using adequate magnetocaloric materials and frequencies, among other parameters. The cooling by sweeping concept can be easily extended to electrocaloric, barocaloric and elastocaloric materials.

Acknowledgement

The present study was developed in the scope of the Smart Green Homes Project [POCI-01-0247-FEDER-007678], a co-promotion between Bosch Termotecnologia S.A. and the University of Aveiro. It is financed by Portugal 2020 under the Competitiveness and Internationalization Operational Program, and by the European Regional Development Fund. Project CICECO-Aveiro Institute of Materials, POCI-01-0145- FEDER-007679 (FCT Ref. UID/CT/5001/2013), financed by national funds through the FCT/MEC

and co-financed by FEDER under the PT2020 Partnership Agreement is acknowledged. JSA acknowledges FCT IF/01089/2015 research grant.

References

References

[1] K. Gschneidner Jr., V. Pecharsky, Thirty years of near room temperature magnetic cooling: Where we are today and future prospects, Int. J. Refrig. 31 (6) (2008) 945.

[2] X. Moya, S. Kar-Narayan, N. D. Mathur, Caloric materials near ferroic phase transitions, Nat. Mater. 13 (5) (2014) 439.

[3] A. Kitanovski, U. Plaznik, U. Tomc, A. Poredoš, Present and future caloric refrigeration and heat-pump technologies, Int. J. Refrig. 57 (2015) 288.

[4] B. Yu, Q. Gao, B. Zhang, X. Meng, Z. Chen, Review on research of room temperature magnetic refrigeration, Int. J. Refrig. 26 (6) (2003) 622.

[5] B. Yu, M. Liu, P. W. Egolf, A. Kitanovski, A review of magnetic refrigerator and heat pump prototypes built before the year 2010, Int. J. Refrig. 33 (2010) 1029.

[6] A. M. Tishin, Y. I. Spichkin, The Magnetocaloric Effect and its Applications, IOP publishing, 1st edn., 2003.

[7] A. Kitanovski, J. Tušek, U. Tomc, U. Plaznik, M. Ožbolt, A. Poredoš, Magnetocaloric Energy Conversion: From Theory to Applications, Springer, Springer Cham Heidelberg New York Dordrecht London, 1st edn., 2015.

[8] V. Franco, J. S. Blázquez, B. Ingale, A. Conde, The magnetocaloric effect and magnetic refrigeration near room temperature: Materials and models, Annu. Rev. Mater. Res. 42 (2012) 305.

[9] I. Niknia, O. Campbell, T. Christiaanse, P. Govindappa, R. Teyber, P. Trevizoli, A. Rowe, Impacts of configuration losses on active magnetic regenerator device performance, Appl. Therm. Eng. 106 (2016) 601–612.

[10] K. Engelbrecht, D. Eriksen, C. R. H. Bahl, R. Bjørk, J. Geyti, J. A. Lozano, K. K. Nielsen, F. Saxild, A. Smith, N. Pryds, Experimental results for a novel rotary active magnetic regenerator, Int. J. Refrig. 35 (6) (2012) 1498.

[11] M. Balli, O. Sari, C. Mahmed, C. Besson, P. Bonhote, D. Duc, J. Forchelet, A pre-industrial magnetic cooling system for room temperature application, Appl. Energy 98 (2012) 556.

[12] J. A. Lozano, M. S. Capovilla, P. V. Trevizoli, K. Engelbrecht, C. R. H. Bahl, J. Barbosa, J. R., Development of a novel rotary magnetic refrigerator, Int. J. Refrig. 68 (2016) 187.

[13] T. Lei, K. Engelbrecht, K. Nielsen, C. Veje, Study of geometries of active magnetic regenerators for room temperature magnetocaloric refrigeration, Appl. Therm. Eng. 111 (2017) 1232–1243.

[14] R. Teyber, P. Trevizoli, T. Christiaanse, P. Govindappa, I. Niknia, A. Rowe, Performance evaluation of two-layer active magnetic regenerators with second-order magnetocaloric materials, Appl. Therm. Eng. 106 (2016) 405–414.

[15] T. Kawanami, S. Hirano, K. Fumoto, S. Hirasawa, Evaluation of fundamental performance on magnetocaloric cooling with active magnetic regenerator, Appl. Therm. Eng. 31 (6-7) (2011) 1176–1183.

[16] J. Wu, B. Lu, C. Liu, J. He, A novel cascade micro-unit regeneration cycle for solid state magnetic refrigeration, Appl. Therm. Eng. 137 (5) (2018) 836.

[17] S. Dall'Olio, T. Lei, K. Engelbrecht, C. Bahl, The effect of tapering on a magnetocaloric regenerator bed, Int. J. Refrig. 84 (2017) 300–308.

[18] U. Tomc, J. Tušek, A. Kitanovski, A. Poredoš, A new magnetocaloric refrigeration principle with solid-state thermoelectric thermal diodes, Appl. Therm. Eng. 58 (2013) 1.

[19] U. Tomc, J. Tušek, A. Kitanovski, A. Poredoš, A numerical comparison of a parallel-plate AMR and a magnetocaloric device with embodied micro thermoelectric thermal diodes, Int. J. Refrig. 37 (1) (2014) 185–193.

[20] W. de Vries, T. van der Meer, Application of Peltier thermal diodes in a magnetocaloric heat pump, Appl. Therm. Eng. 111 (2017) 377–386.

[21] D. J. Silva, B. D. Bordalo, A. M. Pereira, J. Ventura, J. P. Araújo, Solid state magnetic refrigerator, Appl. Energy 93 (2012) 570.

[22] D. J. Silva, J. Ventura, J. P. Araújo, A. M. Pereira, Maximizing the temperature span of a solid state active magnetic regenerative refrigerator, Appl. Energy 113 (2014) 1149.

[23] D. J. Silva, B. D. Bordalo, J. Puga, A. M. Pereira, J. Ventura, J. C. R. E. Oliveira, J. P. Araújo, Optimization of the physical properties of magnetocaloric materials for solid state magnetic refrigeration, Appl. Therm. Eng. 99 (2016) 514.

[24] A. Kitanovski, P. W. Egolf, Innovative ideas for future research on magnetocaloric technologies, Int. J. Refrig. 33 (2010) 449.

[25] K. Nielsen, C. Bahl, K. Engelbrecht, The effect of flow maldistribution in heterogeneous parallel-plate active magnetic regenerators, J. Phys. D: Appl. Phys. 46 (10) (2013) 105002.

[26] T. Petersen, K. Engelbrecht, C. Bahl, B. Elmegaard, N. Pryds, A. Smith, Comparison between a 1D and a 2D numerical model of an active magnetic regenerative refrigerator, J. Phys. D: Appl. Phys. 41 (10) (2008) 105002.

[27] R. Ma, Z. Zhang, K. Tong, D. Huber, R. Kornbluh, Y. Ju, Q. Pei, Highly efficient electrocaloric cooling with electrostatic actuation, Science 357 (6356) (2017) 1130.

[28] J. Tušek, K. Engelbrecht, D. Eriksen, S. Dall'Olio, J. Tušek, N. Pryds, A regenerative elastocaloric heat pump, Nat. Energy 1 (10) (2016) 16134.

[29] R. Bjørk, C. R. H. Bahl, K. K. Nielsen, The lifetime cost of a magnetic refrigerator, Int. J. Refrig. 63 (2016) 48.

[30] N. Roberts, D. Walker, A review of thermal rectification observations and models in solid materials, Int. J. Therm. Sci. 50 (5) (2011) 648.

[31] G. Wehmeyer, T. Yabuki, C. Monachon, J. Wu, C. Dames, Thermal diodes, regulators, and switches: Physical mechanisms and potential applications, Appl. Phys. Rev. 4 (4) (2017) 041304.

[32] J. Kimling, R. Wilson, K. Rott, J. Kimling, G. Reiss, D. Cahill, Spin-dependent thermal transport perpendicular to the planes of Co/Cu multilayers, Phys. Rev. B 91 (14) (2015) 144405.

[33] B. Monfared, Simulation of solid-state magnetocaloric refrigeration systems with Peltier elements as thermal diodes, Int. J. Refrig. 74 (2017) 324.

[34] P. W. Egolf, L. Gravier, T. Francfort, A. G. Pawlowski, G. Courret, M. Croci, High-frequency magnetocaloric modules with heat gates operating with the Peltier effect, Int. J. Refrig. 37 (2014) 176.

[35] E. Pallecchi, Z. Chen, G. Fernandes, Y. Wan, J. Kim, J. Xu, A thermal diode and novel implementation in a phase-change material, Mater. Horizons 2 (1) (2015) 125.

[36] J. B. Puga, B. D. Bordalo, D. J. Silva, M. M. Dias, J. H. Belo, J. P. Araújo, J. C. R. E. Oliveira, A. M. Pereira, J. Ventura, Novel thermal switch based on magnetic nanofluids with remote activation, Nano Energy 31 (2017) 278.

[37] Y. Wang, D. Schwartz, S. Smullin, Q. Wang, M. Sheridan, Silicon Heat

Switches for Electrocaloric Cooling, J. Microelectromech. Syst. 26 (3) (2017) 580.

[38] C. Aprea, G. Cardillo, A. Greco, A. Maiorino, C. Masselli, A comparison between experimental and 2D numerical results of a packed-bed active magnetic regenerator, Appl. Therm. Eng. 90 (2015) 376–383.

[39] S. Lionte, C. Vasile, M. Siroux, Numerical analysis of a reciprocating active magnetic regenerator, Appl. Therm. Eng. 75 (2015) 871–879.

[40] K. Nielsen, K. Engelbrecht, The influence of the solid thermal conductivity on active magnetic regenerators, J. Phys. D: Appl. Phys. 45 (14) (2012) 145001.

[41] Source for the heatrapy package at GitHub, version v0.1.4, `https://github.com/danieljosesilva/heatrapy`, 2017.

[42] D. Silva, J. Amaral, V. Amaral, Heatrapy: A flexible Python framework for computing dynamic heat transfer processes involving caloric effects in 1.5D systems, SoftwareX 7 (2018) 373–382.

[43] T. F. Petersen, N. Pryds, A. Smith, J. Hattel, H. Schmidt, H. J. Høgaard Knudsen, Two-dimensional mathematical model of a reciprocating room-temperature Active Magnetic Regenerator, Int. J. Refrig. 31 (3) (2008) 432.

[44] J. Lyubina, Magnetocaloric materials for energy efficient cooling, J. Phys. D: Appl. Phys. 50 (5) (2017) 053002.

[45] J. Liu, J. D. Moore, K. P. Skokov, M. Krautz, K. Löwe, A. Barcza, M. Katter, O. Gutfleisch, Exploring La(Fe,Si) 13-based magnetic refrigerants towards application, Scr. Mater. 67 (6) (2012) 584.

[46] K. Morrison, J. Lyubina, J. Moore, A. Caplin, K. Sandeman, O. Gutfleisch, L. Cohen, Contributions to the entropy change in melt-spun LaFe11.6Si 1.4, J. Phys. D: Appl. Phys. 43 (13) (2010) 132001.

[47] E. Brück, N. T. Trung, Z. Q. Ou, K. H. J. Buschow, Enhanced magnetocaloric effects and tunable thermal hysteresis in transition metal pnictides, Scr. Mater. 67 (6) (2012) 590.

[48] O. Tegus, E. Brück, L. Zhang, Dagula, K. H. J. Buschow, F. R. De Boer, Magnetic-phase transitions and magnetocaloric effects, Physica B 319 (1) (2002) 174.

[49] H. Yibole, F. Guillou, L. Zhang, N. Van Dijk, E. Brück, Direct measurement of the magnetocaloric effect in MnFe(P,X)(X = As, Ge, Si) materials, J. Phys. D: Appl. Phys. 47 (7) (2014) 075002.

[50] X. Moya, E. Defay, V. Heine, N. Mathur, Too cool to work, Nat. Phys. 11 (3) (2015) 202–205, doi:10.1038/nphys3271.

[51] L. Mañosa, A. Planes, M. Acet, Advanced materials for solid-state refrigeration, J. Mater. Chem. A 1 (16) (2013) 4925.

[52] C. Aprea, A. Greco, A. Maiorino, C. Masselli, Solid-state refrigeration: A comparison of the energy performances of caloric materials operating in an active caloric regenerator, Energy 165 (2018) 439–455.

[53] S. Qian, D. Nasuta, A. Rhoads, Y. Wang, Y. Geng, Y. Hwang, R. Radermacher, I. Takeuchi, Not-in-kind cooling technologies: A quantitative comparison of refrigerants and system performance, Int. J. of Refrig. 62 (2016) 177–192.

[54] A. S. Mischenko, Q. Zhang, J. F. Scott, R. W. Whatmore, N. D. Mathur, Giant electrocaloric effect in thin-film PbZr0.95Ti 0.05O3, Science 311 (5765) (2006) 1270.

[55] J. F. Scott, Electrocaloric materials, Annu. Rev. Mater. Res. 41 (2011) 229.

[56] S. G. Lu, Q. Zhang, Electrocaloric materials for solid-state refrigeration, Adv. Mater. 21 (19) (2009) 1983.

[57] B. Neese, B. Chu, S. G. Lu, Y. Wang, E. Furman, Q. M. Zhang, Large electrocaloric effect in ferroelectric polymers near room temperature, Science 321 (5890) (2008) 821.

[58] S. Qian, L. Yuan, J. Yu, G. Yan, Numerical modeling of an active elastocaloric regenerator refrigerator with phase transformation kinetics and the matching principle for materials selection, Energy 141 (2017) 744–756.

[59] D. Luo, Y. Feng, P. Verma, Modeling and analysis of an integrated solid state elastocaloric heat pumping system, Energy 130 (2017) 500–514.

[60] T. Strässle, A. Furrer, K. A. Müller, Cooling by adiabatic application of pressure - the barocaloric effect, Physica B 276-278 (2000) 944.

[61] P. Lloveras, E. Stern-Taulats, M. Barrio, J. L. Tamarit, S. Crossley, W. Li, V. Pomjakushin, A. Planes, L. Mañosa, N. D. Mathur, X. Moya, Giant barocaloric effects at low pressure in ferrielectric ammonium sulphate, Nat. Commun. 6 (2015) 8801.

[62] L. Mañosa, D. González-Alonso, A. Planes, E. Bonnot, M. Barrio, J. L. Tamarit, S. Aksoy, M. Acet, Giant solid-state barocaloric effect in the Ni-Mn-In magnetic shape-memory alloy, Nat. Mater. 9 (6) (2010) 478.

[63] N. Ma, M. S. Reis, Barocaloric efect on graphene, Sci. Rep. 7 (2017) 13257.

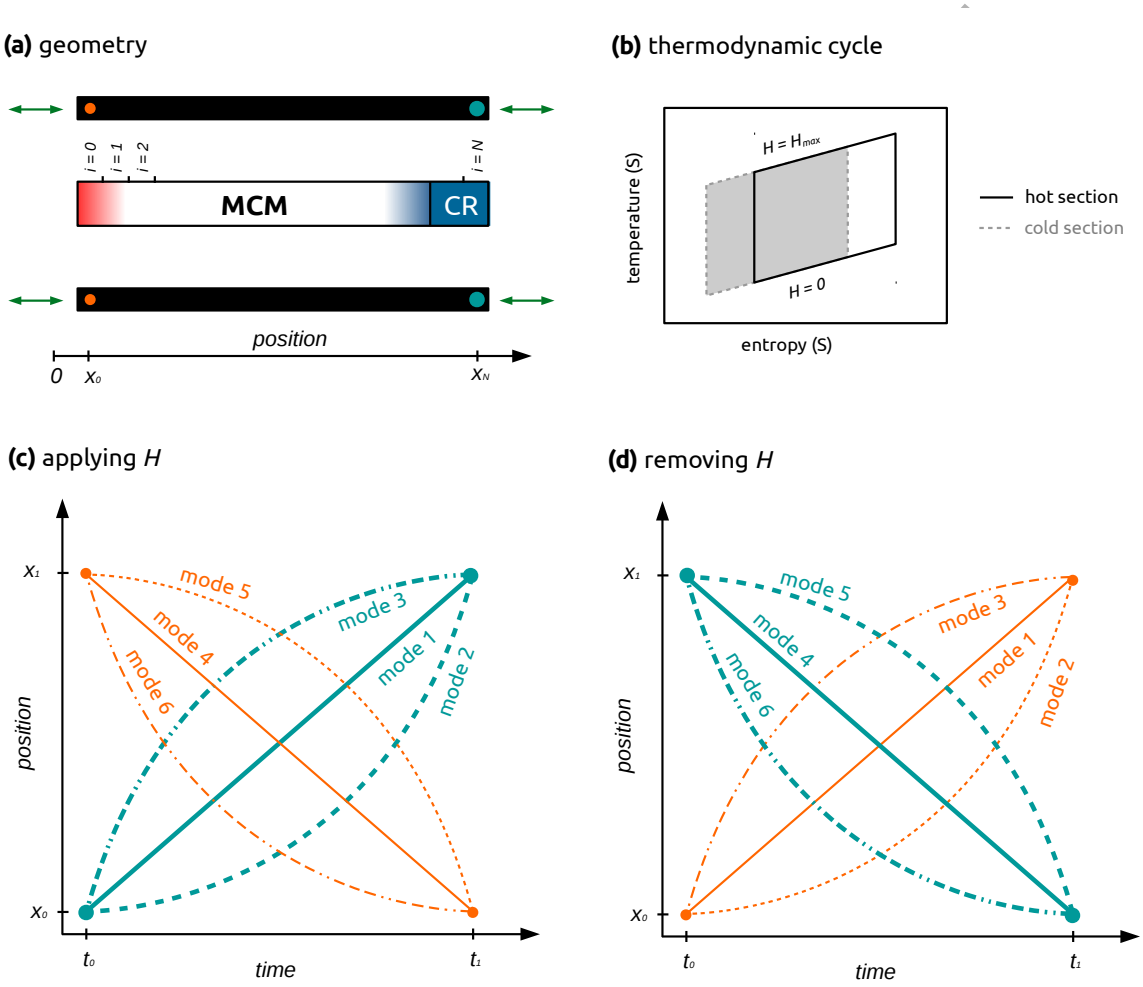

Figure 1: **(a)** 1 dimensional system with the magnetocaloric material (MCM), cold reservoir (CR) and two magnets in black. **(b)** thermodynamic cycle of the nearest sections to the hot and cold reservoirs. The orange (small) and blue (large) circles of the magnets of (a) correspond to probes to describe the motion of the magnets **(b)** during the application of H for the used modes 1-6, and **(c)** during the removal of H for the used modes 1-6.

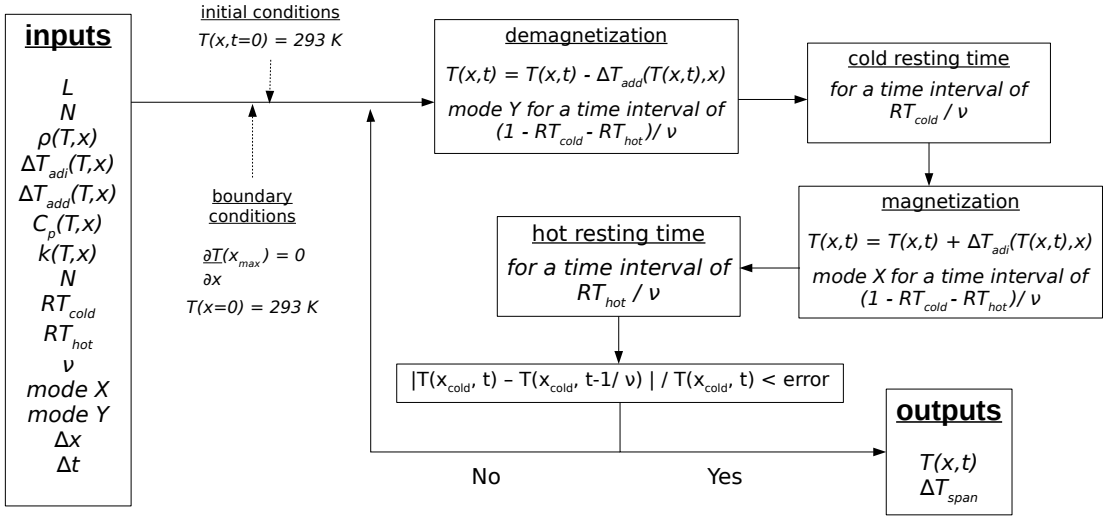

Figure 2: Scheme of the model procedure for running 1 simulation.

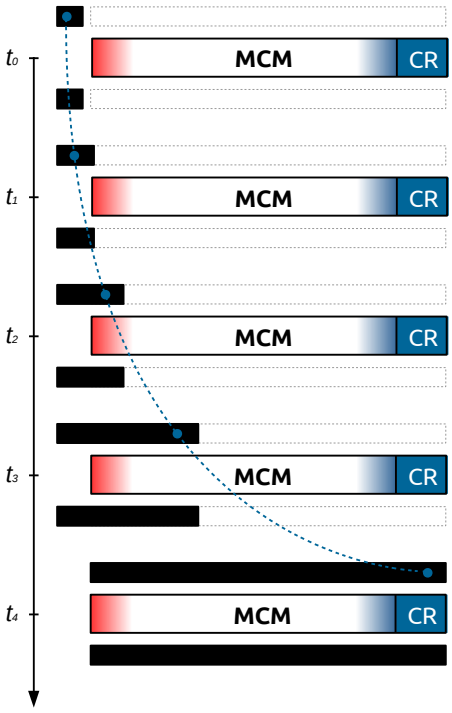

Figure 3: Illustration of the magnet motion for mode 2 (constant acceleration from left to right), starting at t_0 and ending at t_4.

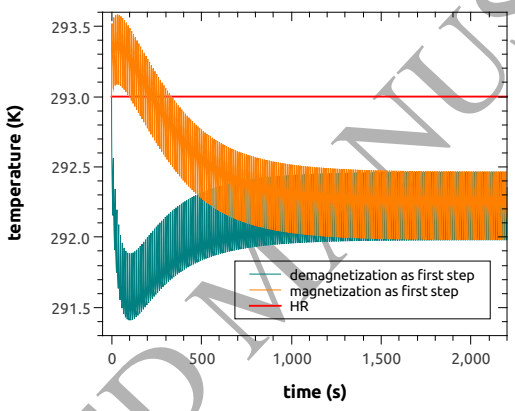

Figure 4: Time evolution of the temperature at the middle of the cold reservoir when using magnetization and demagnetization as fist step for the system operating at mode 56 with $RT_{cold} = 0.5$ and $RT_{hot} = 0.0$. The used operation frequency was 0.1 Hz.

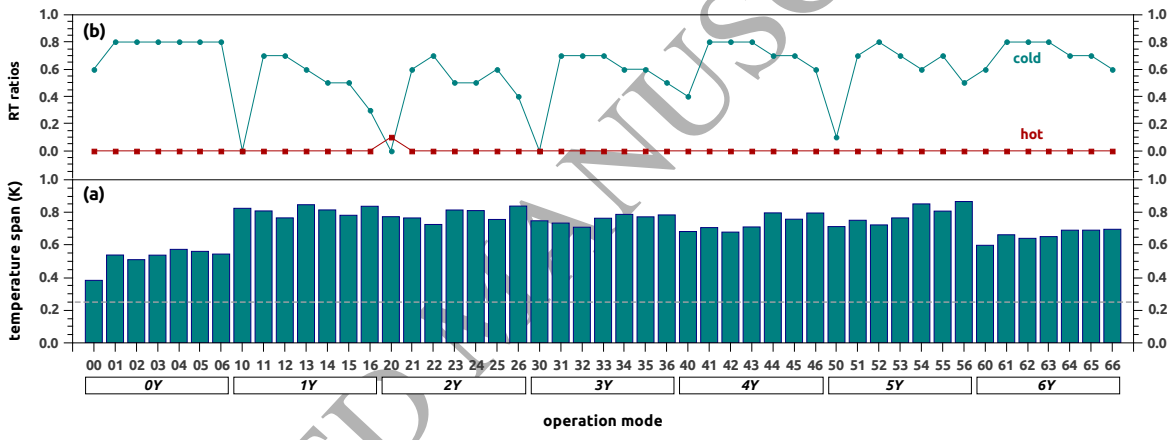

Figure 5: **(a)** Optimized temperature span for all the combinations of operating modes and for demagnetization as first step. The optimization is done for the frequency and for the **(b)** cold and hot resting times. The dashed grey line represents the reference described in the text.